

Structural Effects on Highly Directional Far-Field Emission Patterns of GaN-Based Micro-Cavity Light-Emitting Diodes With Photonic Crystals

Chun-Feng Lai, *Student Member, IEEE*, Hao-Chung Kuo, *Senior Member, IEEE*, Chia-Hsin Chao, Peichen Yu, and Wen-Yung Yeh

Abstract—This study theoretically and experimentally investigates the highly directional far-field emission patterns of GaN photonic crystal (PhC) micro-cavity light-emitting diodes (MCLEDs) depending on varying structural parameters. Angular-spectra-resolved electroluminescence measurements reveals the behavior of guided-mode extraction which is significantly affected by the structural parameters of GaN PhC MCLEDs, where the GaN cavity thickness decides the extracted guided mode numbers, PhC lattice constant influences the distribution of far-field emission, and PhC hole depth affects the interaction with guided modes. The proposed GaN ultrathin MCLED (uMCLED) with PhC lattice constant of 420 nm and deep hole depth of 250 nm exhibited a maximum output light extraction efficiency of 248% under one-watt input power compared to GaN non-PhC uMCLED and produced a directional far-field emission pattern at half intensity near $\pm 17^\circ$. The present results indicate that highly directional light extraction enhancement could contribute to developments of many applications, especially for etendue-limited applications such as pico-projectors.

Index Terms—GaN, light-emitting diodes (LEDs), micro-cavity, photonic crystals (PhCs).

I. INTRODUCTION

LIGHT-EMITTING diodes (LEDs) have recently attracted great concern as a high-saving energy efficiency of lighting technology [1]. Developing next-generation GaN-based LEDs for applications of projecting displays, automobile headlights, and general lightings requires further improvement in light extraction efficiency (LEE) and directionality of far-field emission distribution. GaN micro-cavity (thin-film) LEDs (MCLEDs) are potentially powerful high-brightness LEDs and enable higher power operation due to their excellent thermal

dissipation and electrical conductivity substrate [2], [3]. To extract the guided light of GaN MCLEDs for optimal LEE enhancement, GaN effective cavity length of GaN MCLEDs should be within the micro-cavity regime to support just a few cavity modes so that some cavity modes lying within the extraction cone are leaky to increase the LEE [4]. Nevertheless, a fraction of light power of GaN MCLEDs is still trapped in the GaN waveguide as guided modes. Using the characteristics of PhCs is another way to improve the LEE and directional far-field emission pattern of GaN MCLEDs [5]–[7]. The dependence of the LEE on the micro-cavity and PhC parameters of GaN MCLEDs has been reported by theoretical discussion [8], [9]. However, previous work did not study the structural parameter effects of GaN-based PhC MCLEDs on the directional far-field emission pattern.

This study theoretically and experimentally demonstrates that the LEE and directional far-field emission characteristics of GaN PhC MCLEDs are influenced significantly by several structural parameters, including the GaN cavity thickness T , PhC lattice constant a , and PhC hole depth t . Angular-spectra-resolved electroluminescence (EL) measurement under electrical injection reveals guided-mode extraction behavior depending on the different GaN cavity thickness, PhC lattice constant size, and PhC hole depth.

II. EXPERIMENTS

The blue GaN LED wafers used in this study were grown by metal organic chemical vapor deposition (MOCVD) onto *c*-face (0001) 2-in-diameter sapphire substrates. The GaN LED structure consists of a 30-nm GaN nucleation layer, a 2- μm undoped GaN buffer layer, a 2- μm Si-doped n-GaN layer, a 120 nm InGaIn/GaN MQW active region with 12 periods of 2/8 nm well/barrier width (dominant wavelength $\lambda_o = 455$ nm), a 20-nm Mg-doped p-AlGaIn electron blocking layer, a 125-nm Mg-doped p-GaN contact layer. After epilayer wafer bonding to the Si wafer, the sapphire substrate was removed with the laser lift-off (LLO) technique. Fig. 1 shows the fabrication steps of GaN MCLEDs incorporated with square PhC lattice structures. First, the fabrication process of the GaN LEDs on Si began with the deposition of transparent contact Ni layer (5 nm), silver mirror (130 nm), and Ti/W/Ti/W/Ti/Au bonding metal layer on p-GaN. The GaN LED wafers were then bonded onto a Ti/Pt/Au coated p-type conducting Si substrate by commercial SUSS SB6e wafer bonder. Second, the wafer bonded samples were taken to undergo the LLO process to remove the sapphire

Manuscript received May 03, 2010; revised July 08, 2010; accepted July 15, 2010. Date of publication July 29, 2010; date of current version September 22, 2010.

C. F. Lai is with the Institute of Electro-Optical Engineering, National Chiao Tung University, Hsinchu 300, Taiwan, R.O.C., and also with the Electronics and Opto-electronics Research Laboratories, Industrial Technology Research Institute, Hsinchu 310, Taiwan, R.O.C.

H. C. Kuo and P. Yu are with the Institute of Electro-Optical Engineering, National Chiao Tung University, Hsinchu 300, Taiwan, R.O.C. (e-mail: hckuo@faculty.nctu.edu.tw).

C. H. Chao and W. Y. Yeh are with the Electronics and Opto-electronics Research Laboratories, Industrial Technology Research Institute, Hsinchu 310, Taiwan, R.O.C.

Color versions of one or more of the figures in this paper are available at <http://ieeexplore.ieee.org>.

Digital Object Identifier 10.1109/JLT.2010.2061836

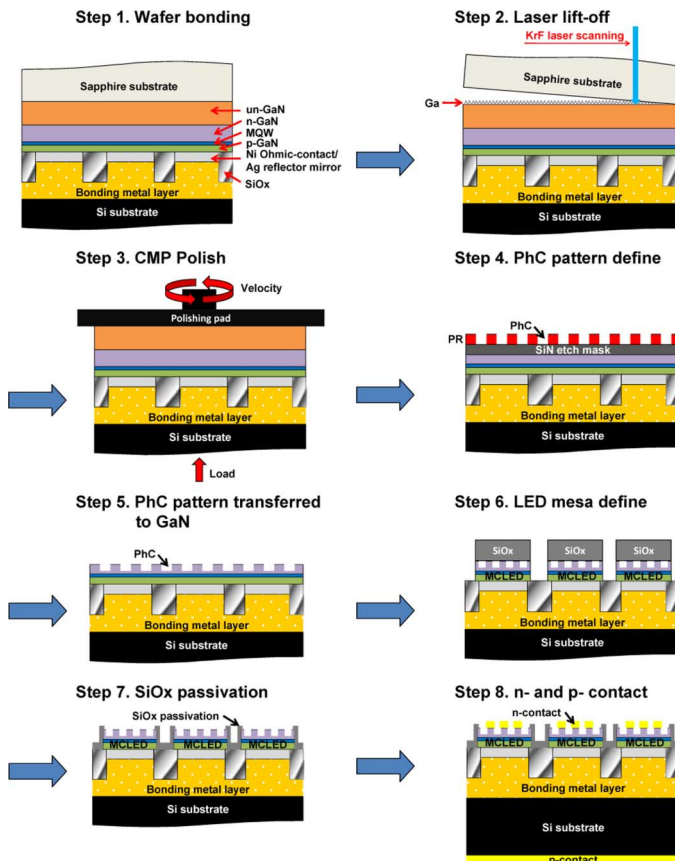


Fig. 1. Schematic diagram of fabrication steps of GaN-based MCLEDs combined with PhC lattice structures.

substrate. In this process, the beam size of KrF laser was larger than our desired size ($1.0 \times 1.0 \text{ mm}^2$) of MCLEDs. Therefore, the laser irradiation on the interface of sapphire and GaN was uniform. After the sapphire removed samples were dipped into HCl solution to remove the residual Ga on the un-GaN. Third, the resulting structure was then thinned down by chemical-mechanical polishing (CMP) to obtain the four GaN micro-cavity thickness T of approximately 3λ ($\sim 560 \text{ nm}$), 4λ ($\sim 740 \text{ nm}$), 8.5λ ($\sim 1580 \text{ nm}$), and 11λ ($\sim 2000 \text{ nm}$), which were measured by α -step profilometer after fabrication. Then the residue was removed with an oxygen reactive ion etch (RIE); this process was found *not* to affect the current spreading over n-GaN layer. Fourth, to fabricate PhCs on the n-GaN surface, a 200-nm-thick layer of SiN was deposited on the n-GaN by plasma-enhanced chemical vapor deposition (PECVD) to serve as a hard mask. The PhC with a square lattice of circular holes was then defined by interference lithography on the hard mask. Fifth, PhC holes were then etched into the top n-GaN surface using inductively coupled plasma (ICP) dry etching to a deep hole depth t of 250 nm. Sixth, the associated mesas ($800 \times 800 \mu\text{m}^2$) were etched to the bonding metal interface to isolate each single chip. Then using a buffer oxidation etchant (BOE) removed the residual SiO_2 layer. Seventh, the SiO_2 was deposited on the sidewall as the passivation layer. Finally, a patterned Cr/Au (50/5000 nm) electrode was deposited on n-GaN to form an n-type contact layer and Cr/Au (5/1000 nm) metal was deposited on back of

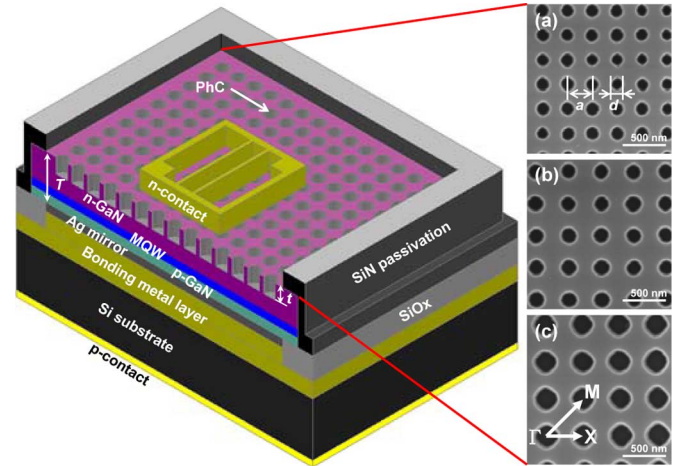


Fig. 2. Schematic diagram of the GaN MCLED structures incorporated with PhC structures. The SEM images of PhC structures were designed to the square lattice nanoholes with lattice constant (a) $a = 270$, (b) $a = 370$, and (c) $a = 420 \text{ nm}$, where the diameter d were fixed to the ratio $d/a = 0.7$.

the Si substrate to form a p-type contact layer. Fig. 2 shows the GaN MCLED structure incorporated with square PhC lattice. According to the previous work as in [6], three different PhC lattice constant a values are 270, 370, and 420 nm and the hole diameter d are fixed to the ratio $d/a = 0.7$ for collimated far-field patterns, their scanning electron microscopy (SEM) images shown in Fig. 2(a)–(c). After dies fabrication, the dies were mounted on the transistor outline (TO-46) package *without* epoxy encapsulation.

III. THEORETICAL MODEL

After sample preparation, the micro-cavity effect on the LEE and far-field emission pattern of planar (non-PhC) GaN MCLEDs was studied. We performed angular-spectra-resolved EL measurement with current injection to investigate the behavior of guided mode extraction and the distribution of far-field emission [10]. Fig. 3(a) shows the angular spectra at various angles from the thick planar GaN MCLED. It fully characterized the far-field emission distribution of thick planar GaN MCLED. The MQW emission of thick planar GaN MCLED is clearly modulated by the Fabry–Perot (FP) effect. The angular spectra of Fig. 3(b) were normalized by the shape of the MQW line, as in [11]. The angular dependent spectra was shown in the general form of $I(\lambda_o, \theta) = \lambda_o \cos(\theta) = (2n_s T/m_c) \cos(\theta)$, where m_c is the cavity mode number, n_s is the refractive index of GaN material, and T is the GaN cavity thickness. The theoretical results showed the GaN cavity thickness of $T = 2.25 \mu\text{m}$, GaN refractive index $n_s = 2.45$, and FP mode number m_c from 20 (green dashed line) to 26 (light yellow dashed line) above the air cone, as shown in Fig. 3(b). These measured results agreed well with the actual structure of GaN MCLED. The 2.25- μm thick planar GaN MCLED has twenty-six resonance modes. Fig. 3(b) reveals only seven FP modes outside the extraction cone, and other resonance modes trapped in the GaN waveguide as guided mode. Additionally, the FP effect modulated the MQW emission of planar GaN MCLED and showed near perfect detuning between the emission wavelength

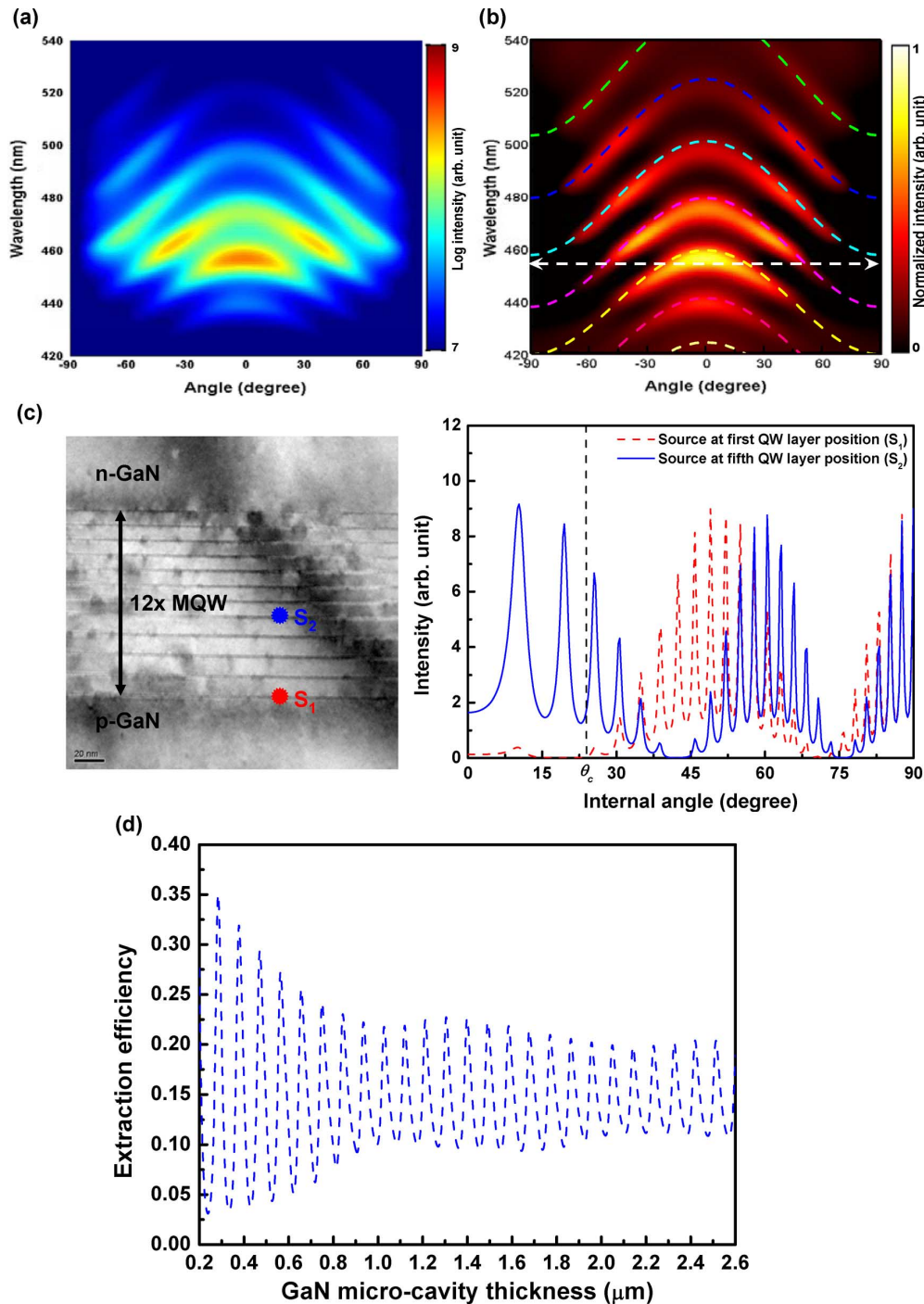


Fig. 3. (a) Un-polarized angular-spectra-resolved EL measurements of the planar GaN MCLED with thickness $T \sim 2.25 \mu\text{m}$ at a driven current of 50 mA. (b) Normalized EL angular spectra for the planar GaN MCLED is the resonant $2.25 \mu\text{m}$ cavity device, the figure inset shows the theoretical fitting results. White dashed line is the MQW dominant emission wavelength. (c) The light intensity emitted from the planar GaN MCLED was calculated by the different source position S_1 and S_2 in the planar GaN MCLED with monochromatic light emitting wavelength of 455 nm. Light emitted outside θ_c (dashed vertical line) is extracted to air. Inset the TEM image of the planar GaN MCLED with 12x InGaN/GaN MQW. (d) LEE of planar GaN MCLED structure is plotted as a function of the GaN cavity thickness T . The dipole source was placed in the position of the fifth QW layer about 186 nm from S_2 to Ag mirror.

(white dashed line with arrows) and the cavity length indicated by divergent emission [11].

According to the micro-cavity theory [4], the GaN cavity thickness T and position of QW layers in the GaN MCLED with bottom metallic reflector mirror is an important factor that strongly modifies light emitting characteristics such as the LEE, spontaneous emission rate, and far-field emission patterns [12],

[13]. The light emission intensity is controlled by two factors. The airy function that indicated transmittance behavior of the FP cavity was controlled by the cavity thickness of GaN, T . The anti-node factor is controlled by the position of QW layers relative to the high-reflectance metal mirror, which governed the coupling efficiency of the light source in guided mode. In this study, the transmission electron microscopy (TEM) image

was used to confirmed epilayers of our GaN MCLEDs that the p-GaN about 145 nm and MQW layer made of 12 periods of 2/8 nm well/barrier width, as shown in Fig. 3(c). Fig. 3(c) inset shows the light intensity emitted from the planar GaN MCLED and reveals two QW positions located at different distances from the Ag mirror. One was placed at the node (S_1) so that the extraction efficiency of MCLED was suppressed; the other was placed at the anti-node (S_2) in the position of the fifth QW layer. The LEE was maximal when the source was located at an anti-node of the given mode. Therefore, each of the QW positions in GaN MCLEDs has to be designed at the optimal distance from the Ag mirror, to improve the extraction efficiency with the micro-cavity effects.

The influence of GaN cavity thickness T on the LEE has been studied numerically in detail though [8], [9]. This study considers the actual device structure that contains the 120-nm MQW and 145-nm p-GaN. The dipole source was placed in the position (S_2) of the fifth QW layer. Fig. 3(d) shows the light extracted out from critical angle $\theta_c (\sim \sin^{-1}(1/n_s))$ of GaN MCLED structures as a function of GaN cavity thickness T . The transmittance curve which is obtained from the formula in [4] depends on the airy function and anti-node factor for a monochromatic light emitting at a wavelength of 455 nm in GaN MCLED structure. The LEE periodically changes with GaN cavity thickness T varying from 0.2 to 2.6 μm . The periodicity of the GaN cavity thickness T is about 93 nm which correspond to $\sim \lambda_o/2n_s$. The peak (valley) of Fig. 3(d) is caused by the constructive (destructive) interference of upward emitted light and downward reflected light that will influence the LEE and distribution of far-field emission. The results reveal that LEE of planar GaN MCLED strongly depends on GaN cavity thickness T of the structural parameters.

IV. EXPERIMENT RESULTS AND DISCUSSION

From the above discussion, the thick planar GaN MCLED still trapped some guided modes in the material. To both increase the LEE and obtain a directional far-field emission pattern from a non-optimized cavity length of planar GaN MCLED, we used the GaN MCLED incorporated with square PhC lattice to enhance the LEE and control the distribution of far-field emission. Many studies have investigated LEE improvement in GaN MCLED with PhC structures [14]–[16]. Furthermore, we will discuss the structural parameters of GaN PhC MCLEDs affecting the distribution of far-field emission.

A. GaN Cavity Thickness Effect

In this section, we studied the different GaN cavity thickness T of GaN PhC MCLEDs influence on the distribution of directional far-field emission using the same PhC lattice constant a and depth of PhC hole t . Angular-spectra-resolved EL measurement under the driven current of 50 mA indicated the GaN PhC MCLED with the PhC lattice constant $a = 420$ nm, PhC hole depth $t = 250$ nm, and two different GaN cavity thicknesses T of about 11λ and 3λ . This is clearly shown in Fig. 4(a) and (b) with light collected along the ΓX (left) and ΓM (right). The shape of the MQW line normalized these angular spectra of GaN PhC MCLED [11]. The light traveling through the waveguide in the GaN PhC MCLEDs was diffracted by reciprocal

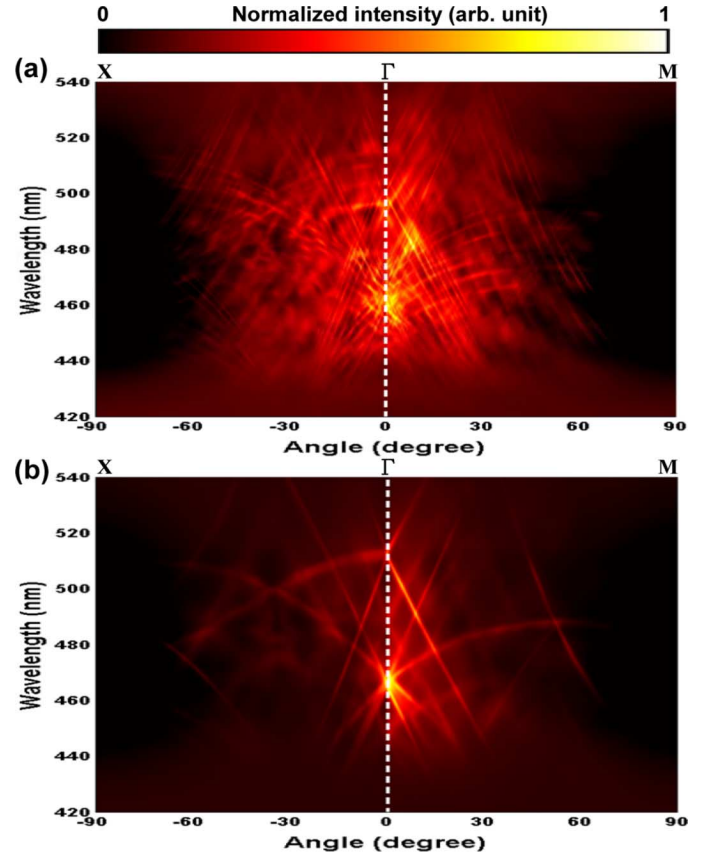


Fig. 4. Un-polarized angular-spectra-resolved EL measurements of the GaN PhC MCLED with PhC lattice constant $a = 420$ nm, and PhC hole depth $t = 250$ nm measured the different GaN cavity thickness (a) $T \sim 11\lambda$ and (b) $T \sim 3\lambda$ under the driven current of 50 mA, where the left shown in ΓX direction and the right in ΓM direction.

wavevectors associated with the square PhC lattice. The sharp lines could be attributed by extracted wave guided modes propagating in the GaN waveguides formed with the GaN cavity thickness between the Ag reflector mirror and the air. Fig. 4(a) shows many guided modes extraction of the thick ($T \sim 11\lambda$) GaN PhC MCLED, in contrast to Fig. 4(b), the GaN PhC ultrathin ($T \sim 3\lambda$) MCLED (uMCLED) is extracted only two guided modes. The extracted guided mode numbers were significantly affected via the GaN cavity thickness T of GaN PhC MCLED. Furthermore, the guided mode dispersion of the thick ($T \sim 11\lambda$) GaN PhC MCLED is still quite close to the free-photons band structure because the PhC diffraction grating only has a perturbative effect on dispersion (the same as previous literatures, these photon bands diagram are not shown) [6], [17]. Nonetheless, GaN PhC uMCLED with $T \sim 3\lambda$ extracts approximately two lower-order guided modes whose dispersion is more strongly affected by PhC hole depth. The photonic dispersion of thin device combining PhC and micro-cavity effects differs significantly from that of the GaN sapphire-based structures [17].

Due to the PhC diffracting these guided modes into the air, they could be quantitatively analyzed using the Ewald construction of the Bragg diffraction theory in reciprocal space [15]. The extraction of waveguided light into air could be described by the relation $|k_{m,\text{eff}} \pm xG| < k_0$, where $k_{m,\text{eff}}$ is a wavevector of the

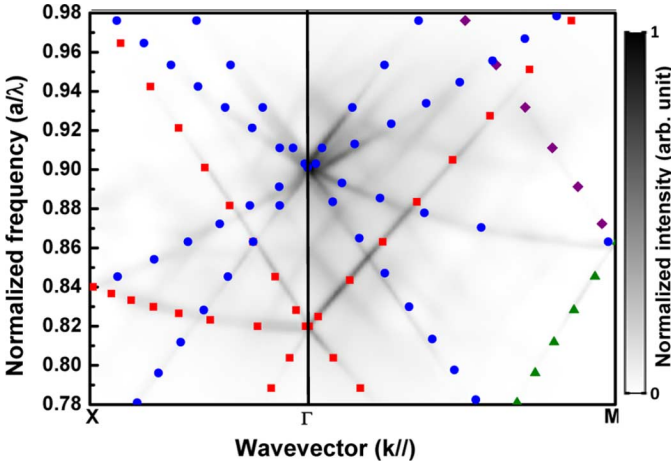


Fig. 5. The guided mode dispersion curves determined from the data shown in Fig. 4(b) and compared with the fundamental mode dispersion curves for the transverse electric (TE) modes.

effective refractive index guided mode, m is the guided mode number, G represents the various reciprocal diffraction vectors (as $G_{\Gamma X}$, $G_{\Gamma M}$, and $G_{\Gamma X1M}$ of square PhC lattice [15]), and $x = 1, 2, \dots$ is an integer, the order of diffraction. The radius of the air circle was $k_o = 2\pi/\lambda_o$. Each waveguide mode circle could be characterized by $k_{m,\text{eff}} = 2n_s\pi/\lambda_o \times \sin(\theta_m)$, where θ_m is internal angle of the guided mode propagation within the GaN waveguide. When the in-plane component of the resultant wavevector after coupling to a reciprocal lattice vector fell within the circle of air, the diffracted light escaped into the air at an angle, $\theta_{m,\text{air}} = \sin^{-1}[(\lambda_o/2\pi)|k_{m,\text{eff}} \pm xG|]$. Therefore, the condition of diffraction depends on the wavelength λ_o , PhC lattice constant a , and guided mode propagation angle θ_m . Each of the guided modes propagates in the GaN waveguide at different angles θ_m due to the MQW emission from the GaN MCLED influenced by the anti-node factor [4], as shown in Fig. 3(c). Therefore, we determined that each guided mode interacts with the PhC differently [5]. To study behavior of these modes more clearly, the spectra shown in Fig. 4(b) were transformed to the guided mode dispersion curves shown in Fig. 5 [17]. The image shows the normalized dispersion curves for each mode line in the ΓX (left) and ΓM (right) directions. To study the observed lines of guided mode, the dispersion of the effective refractive index $n_{m,\text{eff}}(\lambda)$ of fundamental mode ($m = 0$) was calculated by a slab waveguide with the GaN material dispersion formula, a Sellmeier equation [18]. The dispersion curves of the fundamental mode were evaluated by a Bragg diffraction equation as $|k_{o,\text{eff}} \pm xG| < k_o$ [15], where $k_{o,\text{eff}} = 2n_{o,\text{eff}}(\lambda)\pi/\lambda$ was a wavevector of the fundamental mode, $2G_{\Gamma X}$ (square, ■), $G_{\Gamma X1M}$ (circle, ●), $G_{\Gamma M}$ (triangular, ▲), and $2G_{\Gamma M}$ (diamond, ◆) of four diffraction vectors in ΓX and ΓM directions, respectively, of the square PhC lattice, as shown in Fig. 5. These dispersion curves were used to match the observing guided mode lines in Fig. 5. The fundamental guided mode was clearly visible and could be matched to the corresponding dispersion curves of fundamental mode. The results for guided mode dispersion were different with thick GaN PhC MCLEDs, where the dispersion was simply folded free-photon bands.

The waveguided light diffracted through PhC exhibited anisotropy in the far-field pattern, both in the direction of the zenith and the azimuth [6], [15]. The far-field angle is an included angle made by two lines with common vertex (the origin) across the half intensities of the far-field patterns. The far-field emission pattern of GaN PhC MCLED was measured in ΓX (solid line) and ΓM (dashed line) directions of square PhC lattice. To investigate how the GaN cavity thickness T influences the distribution of far-field emission of GaN PhC MCLED, the 3-D far-field radiation pattern of GaN PhC MCLED with different GaN cavity thickness, was measured by means of imaging spheres (Radiant imaging IS-LI) under the same current 50 mA for beam shape comparison, normalized with peak intensity. The measured far-field emission patterns of GaN MCLEDs with different GaN thicknesses T of $\sim 11\lambda$ and $\sim 3\lambda$ were shown in Fig. 6(a) and (b) respectively. From Fig. 6, far-field patterns of non-PhC MCLED plotted in dash-dot lines have far-field angles of about 118.56° and 96.24° in GaN thicknesses of $\sim 11\lambda$ and $\sim 3\lambda$, respectively, which are much lower than that of the typical 120° Lambertian far field distribution due to the strong micro-cavity effect [11]. The GaN PhC MCLEDs with PhC lattice constant $a = 420$ nm and PhC hole depth $t = 250$ nm in thick ($T \sim 11\lambda$) and thin ($T \sim 3\lambda$) GaN thicknesses cause differing far-field emission patterns plotted in solid (dash) lines for ΓX (ΓM) PhC lattice orientation, also shown in Fig. 6(a)–(b). The patterns peaked near normal on the surface of the device with far-field angles at half intensity of 98.72° (80.68°) and 34.23° (41.39°) in ΓX (ΓM) respectively. The ultrathin cavity length of GaN PhC MCLEDs based on two lower-order guided modes revealed the strong influence of micro-cavity on a highly-directional far-field emission pattern. Therefore, the GaN cavity thickness of the structural parameters affects the guided modes extraction behavior and significantly modifies the distribution of the directional far-field emission on GaN PhC MCLED.

B. PhC Lattice Constant Effect

Thinner GaN cavity thickness T of GaN PhC MCLEDs from the above discussion revealed more highly-directional far-field emission patterns. Further, we discussed the PhC structural parameters including lattice constant a and hole depth t in GaN PhC MCLEDs affecting the directional far-field emission distributions. In this section, we studied the influence of different PhC lattice constant a of GaN PhC MCLEDs on the distribution of directional far-field emission using the same GaN cavity thickness T and PhC hole depth t . The far-field emission distributions of thick ($T \sim 8.5\lambda$) GaN PhC MCLEDs were significantly modified by the PhC lattice constant a [6]. This study discussed thicker ($T \sim 11\lambda$) GaN PhC MCLEDs with various PhC lattice constants.

Angular-spectra-resolved EL measurement under the driven current of 50 mA for GaN PhC MCLEDs with thick GaN cavity thickness $T \sim 11\lambda$, PhC hole depth $t = 250$ nm, and two different PhC lattice constant $a = 270$ and 370 nm are shown in Fig. 7(a) and (b) with light collected along the ΓX (left) and ΓM (right), respectively. In Fig. 7(a)–(b), many guided modes extraction due to a stronger effects of thick GaN cavity thickness and lattice constant a can be observed, like the Fig. 4(a) with the

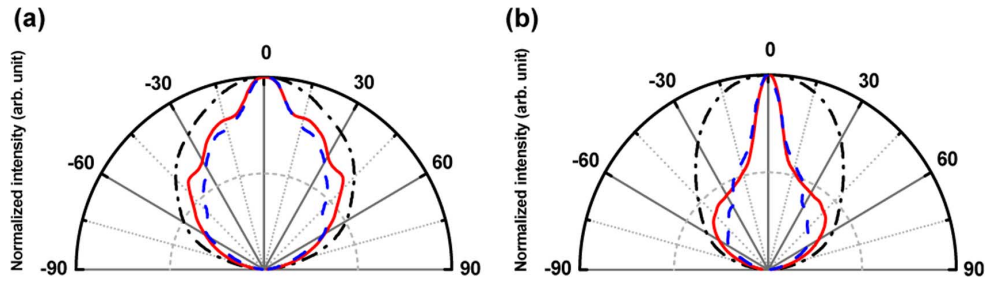


Fig. 6. The far-field emission patterns of GaN PhC MCLEDs with various GaN cavity thickness (a) $T \sim 11\lambda$ and (b) $T \sim 3\lambda$. Solid line is ΓX direction, dashed line is ΓM direction, and dash-dot line is non-PhC.

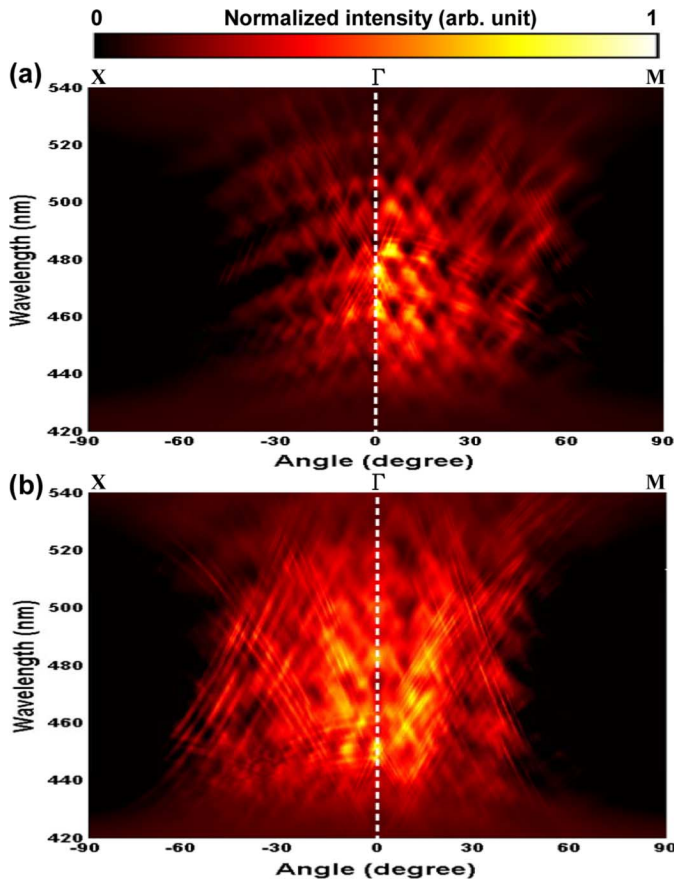


Fig. 7. Un-polarized angular-spectra-resolved measurements of the GaN PhC MCLED with 11λ GaN cavity thickness and PhC hole depth $t = 250$ nm measured the different PhC lattice constant (a) $a = 270$ and (b) 370 nm at a driven current 50 mA, where ΓX is left and ΓM is right direction.

same cavity thickness $T \sim 11\lambda$. The guided mode dispersion of Fig. 7(a) and 7(b) are close to the free-photons band structures. The FP modes in Fig. 7(a) is more clear than in Fig. 7(b). This is because trapped light was extracted more by the PhC with larger lattice constant $a = 370$ nm due to more light coupling directions [15], which make FP modes behind the extracted guided modes.

To investigate how the PhC lattice constant a influences the distribution of far-field emission of GaN PhC MCLED with the same GaN cavity thickness $T \sim 11\lambda$ and PhC hole depth $t = 250$ nm, the far-field radiation patterns of GaN PhC MCLED under the driven current of 50 mA, with the different PhC lattice constant shown in Fig. 8(a)–(b) were measured. Results show the differing far-field emission patterns peaked near normal on

the surface of the device with far-field angles of 74.9° (93.3°) and 112.6° (88.39°) in ΓX (ΓM), respectively. Although experimental results did not reveal highly-directional far-field emission patterns of thick GaN PhC MCLEDs, it was also observed significantly modified by the PhC lattice constant a .

C. PhC Hole Depth Effect

This section discussed the influence of different PhC hole depth t of GaN PhC uMCLED on the distribution of directional far-field emission using the same GaN cavity thickness T and PhC lattice constant a . Angular-spectra-resolved EL measurement under the driven current of 50 mA indicates GaN PhC uMCLED with a square PhC lattice constant of $a = 370$ nm, and two different PhC hole depths, where the shallow and deep etching of the PhC hole depth were about 100 nm and 250 nm. This is clearly shown in Fig. 9(a)–(b) with light collected along the ΓX (left) and ΓM (right). The light traveling through the waveguided in the GaN PhC uMCLEDs was diffracted by reciprocal wavevectors associated with the PhC structures. Observations of the shallow PhC etching of GaN PhC uMCLEDs revealed only two lower-order guided mode extractions, as shown in Fig. 9(a). In contrast, Fig. 9(b) illustrated the deep PhC etching of GaN PhC uMCLEDs in nearly single guided mode extraction. The photon band structures of Fig. 9(a)–(b) agreed with the dispersion curves of the guided mode effective refractive index. There have been discussed carefully elsewhere as [19]. The photon band structure results in this study differ from those in previous works, which showed shallow PhC etching of thick GaN PhC MCLEDs and dispersion that was simply the results of folded free-photon bands [6], [17].

To investigate how the PhC hole depth t influence the distribution of far-field emission of GaN PhC uMCLED, this study measured the far-field radiation pattern under the driven current of 50 mA, as shown in Fig. 10(a)–(b). The shallow (~ 100 nm) and deep (~ 250 nm) PhC hole depth t of the GaN PhC uMCLEDs caused differing far-field emission patterns. The patterns peaked near normal on the surface of the device with far-field angles of 120.54° (84.88°) and 30.75° (34.38°) in ΓX (ΓM) respectively. The deep PhC hole of GaN PhC MCLEDs based on near single lower-order guided modes and the strong influence of micro-cavity caused a highly-directional far-field emission pattern. Therefore, the depth of the PhC hole t , PhC lattice constant a , and GaN cavity thickness T , that affected the behavior of guided mode extraction, had significantly modified the distribution of the directional far-field emission of GaN PhC uMCLED.

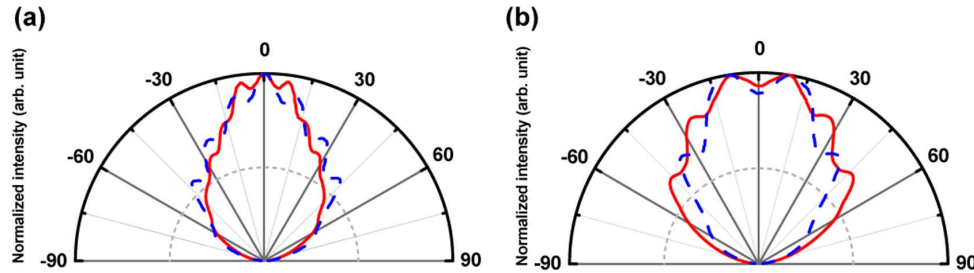


Fig. 8. The far-field emission patterns of GaN PhC MCLED with the cavity thickness of $T \sim 11\lambda$ shows various PhC lattice constant (a) $a = 270$ and (b) 370 nm. Solid line is ΓX direction and dashed line is ΓM direction.

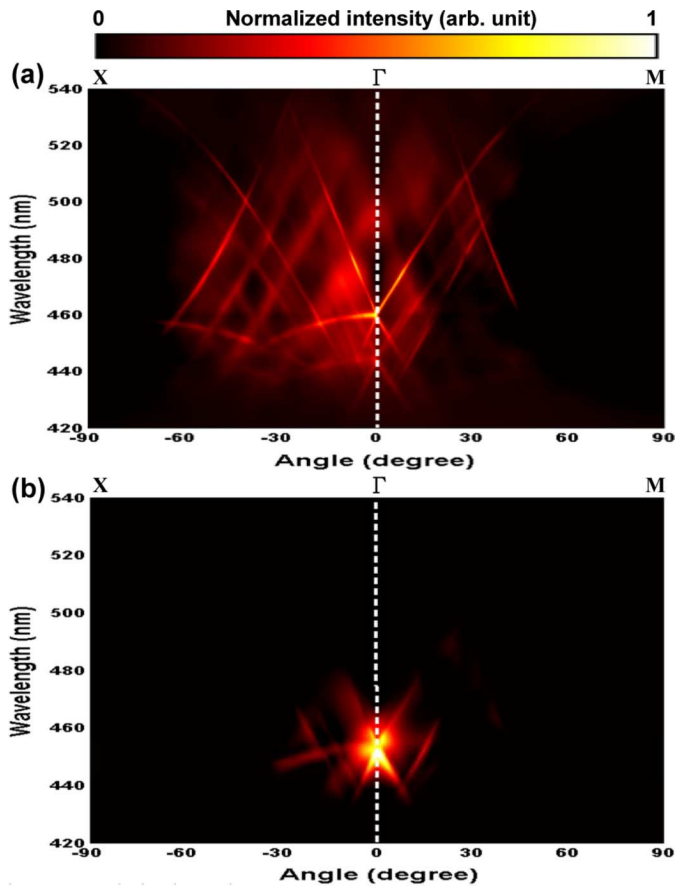


Fig. 9. Un-polarized angular-spectra-resolved measurements of the GaN PhC uMCLED with 3λ GaN cavity thickness and PhC lattice constant $a = 370$ nm measured the different PhC hole depth (a) shallow $t = 100$ nm and (b) deep $t = 250$ nm under the driven current 50 mA, where ΓX is left and ΓM is right direction.

D. Light Extraction Efficiency Discussion

After sample fabrication, we measured the light emission characteristics of the brightness and color uniformity using imaging colorimeters and photometers (Radiant imaging PM-1600F). Fig. 11(a)–(b) shows the optical micrography of GaN uMCLED ($T \sim 3\lambda$) with and without PhC lattice constant $a = 420$ nm under the lower driven current of 1 mA. They uniformly distributed across the chip area by the blue light distribution. It is noteworthy that the current spread under the low injection current could be not affected by the ultrathin GaN

cavity thickness due to the high electron mobility of n-GaN. In addition, the GaN PhC uMCLEDs exhibited a strong LEE, compared with the GaN non-PhC uMCLEDs with the same cavity thickness.

The experiments in this study the absolute light output power-current-voltage ($L-I-V$) characteristics were also measured using an integration sphere with back-thinned charge coupled device (CCD) detector (CAS 140CT—the standard for array spectrometers). The turn-on voltage of the devices was about 2.8 V. This high forward voltage is due to the p-ohmic contact (Ni/Ag) agglomeration caused by high series resistance. The measured external quantum efficiency (EQE) decreased monotonically at current density values larger than 3.125 A/cm² ($\text{EQE}_{\text{max}} \sim 20\%$), because the non-optimized chip processes may suffer current crowding at high current. We considered the above poor characteristics of devices; therefore, Fig. 11(c) shows the absolute light output power of GaN MCLEDs with and without PhC as function of GaN cavity thickness T under the electrical input power of 1 watt (W). The absolute light output power of the GaN PhC MCLEDs with GaN cavity thickness T variation at 3λ (~ 560 nm), 4λ (~ 740 nm), 8.5λ (~ 1580 nm), 11λ (~ 2000 nm), and the PhC lattice constant $a = 420$ nm under the electrical input power of 1 W were enhanced by 248% , 245% , 197% , and 168% , compared with the GaN non-PhC MCLED as shown in Fig. 11(c). This figure clearly shows that the GaN PhC MCLED has a higher light output power than the GaN non-PhC MCLED. The LEE of GaN cavity thickness T variation in GaN non-PhC MCLEDs was also influenced by micro-cavity effect, as shown in Fig. 11(c). In addition, the LEE of GaN PhC MCLED with fixed PhC hole depth $t = 250$ nm strongly depends on the thin GaN cavity thickness T and PhC lattice constant a on the n-GaN layer. A larger PhC lattice constant creates high output power due to more light coupling directions [14]–[16]. In summary, the GaN cavity thickness T , PhC lattice constant a and PhC hole depth t variation significantly modify the light extraction enhancement and directional far-field emission pattern. For highly directional light extraction enhancement, structural parameters including the GaN ultrathin cavity thickness ($T < 3\lambda$), larger PhC lattice constant ($a > 420$ nm), and deep PhC holes ($t \sim$ approaching MQW layer) are optimized to achieve the LED with both high LEE and collimating far fields. Therefore, the study make the highly directional LED promising for entendue-limited application, like pico-projectors [20].

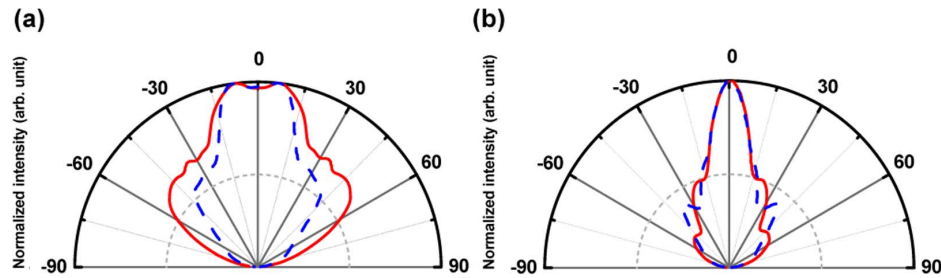


Fig. 10. The far-field emission patterns of GaN PhC uMCLED shows the PhC lattice constant $a = 370$ with different hole depth (a) shallow $t = 100$ nm and (b) deep $t = 250$ nm. Solid line is Γ X direction and dashed line is Γ M direction.

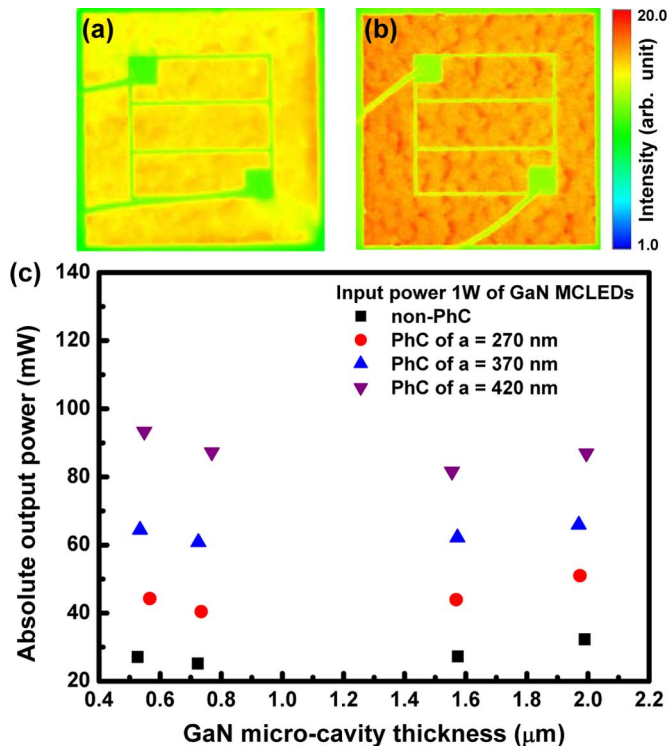


Fig. 11. The colorimeter of optical micrograph showing the blue light distribution across the GaN uMCLED for (a) non-PhC and (b) with PhC lattice constant $a = 420$ nm operated under the low injection current 1 mA, respectively. (c) Light output power characteristics of the GaN MCLLED with and without PhC as function of GaN cavity thickness.

V. CONCLUSION

In conclusion, this study conducted experiment and a theoretical investigation into highly-directional far-field emission patterns of GaN-based PhC MCLLEDs with various structure parameters. Angular-spectra-resolved EL measurements showed the guided modes extraction behavior that were strongly affected by the structural parameters of GaN PhC MCLLED, where GaN cavity thickness influenced the extracted guided mode numbers, PhC lattice constant affected the far-field emission distribution, and PhC hole depth affected the PhC interaction with guided modes. The GaN PhC MCLLED with the ultrathin cavity thickness $T \sim 3\lambda$, PhC lattice constant $a = 420$ nm and deep PhC hole depth $t = 250$ nm exhibited a maximum output LEE of 248% compared to GaN non-PhC MCLLEDs, and produced a highly-directional far-field emission pattern at

half intensity near $\pm 17^\circ$. Highly-directional far-field emission patterns have been demonstrated in an optimized structure. The results indicated that the highly-directional light enhancement of GaN PhC uMCLEDs makes them promising candidates for etendue-limited applications, such as projecting displays.

REFERENCES

- [1] M. R. Krames, O. B. Shchekin, R. Mueller-Mach, G. O. Mueller, L. Zhou, G. Harbers, and M. G. Craford, "Status and future of high-power light-emitting diodes for solid-state lighting," *J. Display Technol.*, vol. 3, no. 2, pp. 160–175, Jun. 2007.
- [2] O. B. Shchekin, J. E. Epler, T. A. Trottier, T. Margalith, D. A. Steigerwald, M. O. Holcomb, P. S. Martin, and M. R. Krames, "High performance thin-film flip-chip InGaN-GaN light-emitting diodes," *Appl. Phys. Lett.*, vol. 89, 2006, Art. ID 071109.
- [3] H. K. Cho, S. K. Kim, D. K. Bae, B. C. Kang, J. S. Lee, and Y. H. Lee, "Laser lift-off GaN thin-film photonic crystal GaN-based light-emitting diodes," *IEEE Photon. Technol. Lett.*, vol. 20, no. 24, pp. 2096–2098, Dec. 2008.
- [4] H. Benisty, H. D. Neve, and C. Weisbuch, "Impact of planar micro-cavity effects on light extraction-Part I: Basic concepts and analytical trends," *IEEE J. Quantum Electron.*, vol. 34, no. 9, pp. 1612–1631, Sep. 1998.
- [5] J. J. Wierer, A. David, and M. M. Megens, "III-nitride photonic-crystal light-emitting diodes with high extraction efficiency," *Nature Photon.*, vol. 3, pp. 163–169, 2009.
- [6] C. F. Lai, C. H. Chao, H. C. Kuo, H. H. Yen, C. E. Lee, and W. Y. Yeh, "Directional light extraction enhancement from GaN-based film-transferred photonic crystal light-emitting diodes," *Appl. Phys. Lett.*, vol. 94, 2009, Art. ID 123106.
- [7] K. Bergeneck, C. Wiesmann, H. Zull, C. Rumbolz, R. Wirth, N. Linder, K. Streubel, and T. F. Krauss, "Strong high order diffraction of guided modes in micro-cavity light-emitting diodes with hexagonal photonic crystals," *IEEE J. Quantum Electron.*, vol. 45, no. 12, pp. 1517–1523, Dec. 2009.
- [8] H. Y. Ryu, "Modification of the light extraction efficiency in micro-cavity vertical InGaN light-emitting diode structures," *J. Kor. Phys. Soc.*, vol. 55, p. 1267, 2009.
- [9] H. Y. Ryu and J. I. Shim, "Structural parameter dependence of light extraction efficiency in photonic crystal InGaN vertical light-emitting diode structures," *IEEE J. Quantum Electron.*, vol. 46, no. , pp. 714–720, May 2010.
- [10] Y. S. Choi, M. Iza, E. Matioli, G. Koblmuller, J. S. Speck, C. Weisbuch, and E. L. Hu, "Submicron-thick microcavity InGaN light emitting diodes," *Proc. SPIE*, vol. 6910, p. 69100R, 2008.
- [11] P. M. Pattison, A. David, R. Sharma, C. Weisbuch, S. DenBaars, and S. Nakamura, "Gallium nitride based microcavity light emitting diodes with 2λ effective cavity thickness," *Appl. Phys. Lett.*, vol. 90, 2007, Art. ID 031111.
- [12] D. Ochoa, R. Houdre, R. P. Stanley, C. Dill, U. Oesterle, and M. Ilegems, "Device simultaneous determination of the source and cavity parameters of a microcavity light-emitting diode," *J. Appl. Phys.*, vol. 85, p. 2994, 1999.
- [13] Y. C. Shen, J. J. Wierer, M. R. Krames, M. J. Ludowise, M. S. Misra, F. Ahmed, A. Y. Kim, G. O. Mueller, J. C. Bhat, S. A. Stockman, and P. S. Martin, "Optical cavity effects in InGaN/GaN quantum-well-heterostructure flip-chip light-emitting diodes," *Appl. Phys. Lett.*, vol. 82, p. 2221, 2003.

- [14] A. David, H. Benisty, and C. Weisbuch, "Optimization of light-diffracting photonic-crystals for high extraction efficiency LEDs," *J. Display Technol.*, vol. 3, no. 2, pp. 133–148, Jun. 2007.
- [15] C. F. Lai, J. Y. Chi, H. C. Kuo, H. H. Yen, C. E. Lee, C. H. Chao, W. Y. Teh, and T. C. Lu, "Far-field and near-field distribution of gan-based photonic crystal leds with guided mode extraction," *IEEE J. Sel. Top. Quantum Electron.*, vol. 15, no. 4, pp. 1234–1241, Jul./Aug. 2009.
- [16] C. Wiesmann, K. Bergenek, N. Linder, and U. T. Schwarz, "Photonic crystal LEDs—Designing light extraction," *Laser Photon. Rev.*, pp. 1–25, 2008.
- [17] A. David, C. Meier, R. Sharma, F. S. Diana, S. P. DenBaars, E. Hu, S. Nakamura, C. Weisbuch, and H. Benisty, "Photonic bands in two-dimensionally patterned multimode GaN waveguides for light extraction," *Appl. Phys. Lett.*, vol. 87, 2005, Art. ID 101107.
- [18] M. Bass, *Handbook of Optics, vol. 2: Devices, Measurements, and Properties*, 2nd ed. New York: McGraw-Hill, 1995.
- [19] C. F. Lai, H. C. Kuo, P. Yu, T. C. Lu, C. H. Chao, H. H. Yen, and W. Y. Yen, "Highly-directional emission pattern based on near single guided mode extraction from GaN-based ultrathin microcavity light-emitting diodes with photonic crystals," *Appl. Phys. Lett.*, vol. 97, 2010, Art. ID 013108.
- [20] F. Fournier and J. Rolland, "Design methodology for high brightness projectors," *J. Display Technol.*, vol. 4, no. 1, pp. 86–91, Mar. 2008.

Chun-Feng Lai (S'10) received the Ph.D. degree in photonics from the Institute of Electro-Optical Engineering, Chiao Tung University, Hsinchu, Taiwan, in 2010.

Since 2010, he has been with Electronic and Opto-Electronics Research Laboratories, Industrial Technology Research Institute, Hsinchu, Taiwan. His current research is focused on high-efficiency GaN-based LEDs and GaN microcavity LEDs via photonic crystals.

Hao-Chung Kuo (M'98–SM'06) received the B.S. degree in physics from National Taiwan University, Taipei, Taiwan, the M.S. degree in electrical and computer engineering from Rutgers University, New Brunswick, NJ, in 1995, and the Ph.D. degree from the Electrical and Computer Engineering Department, University of Illinois at Urbana Champaign, Urbana, in 1999.

Since October 2002, he has been with the National Chiao Tung University (NCTU), Hsinchu, Taiwan, as a Faculty Member of the Institute of Electro-Optical Engineering. He is now the Associate Dean, Office of International Affairs, NCTU. His current research interests include semiconductor lasers, VCSELs, blue and UV LED lasers, quantum-confined optoelectronic structures, optoelectronic materials, and solar cells. He has authored and coauthored 140 internal journal papers and six granted and ten pending patents.

Prof. Kuo is an associate editor of the *JOURNAL OF LIGHTWAVE TECHNOLOGY* and the special issue of the *IEEE JOURNAL OF SELECTED TOPICS IN QUANTUM ELECTRONICS* on "Solid-State Lighting." He was the recipient of the Ta-You Wu Young Scholar Award from the National Science Council and the Young Photonics Researcher Award in 2007.

Chia-Hsin Chao received the B.S.E.E. and Ph.D. degrees from National Sun Yat-Sen University, Kaohsiung, Taiwan, in 1999 and 2006, respectively.

From 2005 to 2006, he was a Visiting Scholar with the Electrical and Computer Engineering Department, University of Illinois at Urbana-Champaign, Urbana. Since 2006, he has been with the Electronic and Opto-Electronics Research Laboratories, Industrial Technology Research Institute, Hsinchu, Taiwan. He is now a Project Deputy Manager and working on photonic crystal LEDs and LED micro-display. His research interests are in the area of numerical electromagnetic field analysis, photonic crystals, and surface plasmon.

Peichen Yu received the B.S. degree in electrophysics and M.S. degree in electrooptical engineering from National Chiao-Tung University, Hsinchu, Taiwan, in 1996 and 1998, respectively, and the Ph.D. degree in electrical engineering from the University of Michigan, Ann Arbor, in 2004.

She was a Design Engineer with the Advanced Design Group, Intel Corporation, Hillsboro, OR, for two years. Her main responsibilities were OPC-related design rule definition and OPC algorithm development of the diffusion layer for the CMOS 65-nm and 45-nm nodes. She joined the Department of Photonics, National Chiao-Tung University as an Assistant Professor in August 2006. Her current research interests include the design and development of photonic crystal-based and quantum dot-based semiconductor devices.

Wen-Yung Yeh received the Ph.D. degree in materials science and engineering from National Tsing Hua University, Taiwan, in 2001.

He is now the Deputy Director of the Opto-electronic Device and System Application Division, Electronics and Opto-electronics Research Laboratories, Industrial Technology Research Institute, Hsinchu, Taiwan. His current research interests include photonic crystal LED, AC LED, and GaN solar cells. He leads the AC LED research team.

Dr. Yeh was the recipient of the R&D 100 Award in 2008.